Letter

Identifying the spin-trapped character of the ^{32}Si isomeric state

J. Williams [1,*] G. Hackman,[1] K. Starosta,[2] R. S. Lubna,[3] Priyanka Choudhary,[4] P. C. Srivastava,[4] C. Andreoiu,[2] D. Annen,[2] H. Asch,[5] M. D. H. K. G. Badanage,[2] G. C. Ball,[1] M. Beuschlein,[6] H. Bidaman,[7] V. Bildstein,[7] R. Coleman,[7] A. B. Garnsworthy,[1] B. Greaves,[7] G. Leckenby,[1,8] V. Karayonchev,[1,†] M. S. Martin,[5] C. Natzke,[1] C. M. Petrache,[9] A. Radich,[7] E. Raleigh-Smith,[1] D. Rhodes,[1] R. Russell,[10] M. Satrazani,[11] P. Spagnoletti,[2] C. E. Svensson,[7] D. Tam,[5] F. Wu (吴桐安),[2] D. Yates,[1,8] and Z. Yu[2]

[1]*TRIUMF, 4004 Wesbrook Mall, Vancouver, British Columbia V6T 2A3, Canada*
[2]*Department of Chemistry, Simon Fraser University, 8888 University Drive, Burnaby, British Columbia V5A 1S6, Canada*
[3]*Facility for Rare Isotope Beams, Michigan State University, 640 South Shaw Lane, East Lansing, Michigan 48824, USA*
[4]*Department of Physics, Indian Institute of Technology Roorkee, Roorkee 247667, India*
[5]*Department of Physics, Simon Fraser University, 8888 University Drive, Burnaby, British Columbia V5A 1S6, Canada*
[6]*Technische Universität Darmstadt, Department of Physics, Institute for Nuclear Physics, Schlossgartenstr. 9, Darmstadt 64289, Germany*
[7]*University of Guelph, 50 Stone Rd E, Guelph, Ontario N1G 2W1, Canada*
[8]*Department of Physics and Astronomy, University of British Columbia, Vancouver, British Columbia V6T 1Z1, Canada*
[9]*Université Paris-Saclay, CNRS/IN2P3, IJCLab, Orsay 91405, France*
[10]*University of Surrey, Guildford GU2 7XH, United Kingdom*
[11]*University of Liverpool, Liverpool L69 3BX, United Kingdom*

(Received 3 August 2023; revised 25 October 2023; accepted 8 November 2023; published 27 November 2023)

The properties of a nanosecond isomer in ^{32}Si, disputed in previous studies, depend on the evolution of proton and neutron shell gaps near the island of inversion. We have placed the isomer at 5505.2(2) keV with $J^\pi = 5^-$, decaying primarily via an $E3$ transition to the 2_1^+ state. The $E3$ strength of 0.0841(10) W.u. is unusually small and suggests that this isomer is dominated by the $(\nu d_{3/2})^{-1} \otimes (\nu f_{7/2})^1$ configuration, which is sensitive to the $N = 20$ shell gap. A newly observed 4_1^+ state is placed at 5881.4(13) keV; its energy is enhanced by the $Z = 14$ subshell closure. This indicates that the isomer is located in a yrast trap, a feature rarely seen at low mass numbers.

DOI: 10.1103/PhysRevC.108.L051305

Neutron-rich nuclides around the $N = 20$ island of inversion contain rich information on nuclear structure. For Na and Mg isotopes, residual nucleon-nucleon interactions lead to the disappearance of the $N = 20$ shell gap and substantial occupation of neutron fp shell orbitals in the ground-state configuration [1–3]. For nearby nuclides in the neutron-rich sd shell, the evolution of the $N = 20$ shell closure is indicated by intermediate energy negative parity states, which arise mainly due to single neutron excitation to the higher-lying fp orbitals. Furthermore, the energies of normal (positive parity) configurations are affected by subshell closures within the sd shell. These differing excitation modes affect the energy spacing and ordering of normal and intruder configurations, influencing the decay scheme of the nucleus and potentially giving rise to nuclear isomerism. Various studies have identified isomers near the island of inversion and have highlighted their importance for understanding the evolving structure in this region [4–6].

For isomers in sd shell nuclei, various systematic trends are apparent from existing data [7]. Spin isomers (where decays are hindered by large ΔJ values, typically $\Delta J \geqslant 3$) are rare in this region and all occur in odd-Z odd-N nuclei near stability, except for two disputed cases in ^{26}F and ^{32}Si. The case of ^{32}Si is particularly interesting due to its proximity to the island of inversion, as well as the fact that it is an even-Z even-N nucleus, and no spin isomers have been identified in even-even nuclei below ^{54}Fe [7]. The scarcity of these isomers in low mass nuclei is due to the absence of intruder orbitals near the Fermi energy that would facilitate high spin states at low excitation energies. For higher mass nuclei near shell closures, spin isomers are common due to the population of high-j intruder orbitals such as $0g_{9/2}$ or $0h_{11/2}$ [7]. In principle, neutron cross-shell excitation to the $0f_{7/2}$ orbital could produce similar isomers in even-even sd shell nuclei near $N = 20$. These isomers could arise either due to small energy gaps between normal and intruder states of similar spin, which hinder transitions between those states, or due to the inversion of the yrast sequence such that a high spin state becomes lower in energy than lower spin states, resulting in a yrast trap that restricts the decay of the higher spin state.

These considerations have brought our attention to ^{32}Si, the lowest mass even-even nucleus in which a spin isomer candidate has been reported. Initially, a $5^- \to 4^+ \to 2_1^+$ cascade was proposed with a small $5^- \to 4^+$ decay energy leading to isomerism of the 5^- state with $\tau_{\mathrm{mean}} \approx 40$ ns [8]. However,

*ewilliams@triumf.ca
†Present address: Argonne National Laboratory, 9700 S. Cass Avenue, Lemont, Illinois 60439, USA.

a subsequent report did not observe the $5^- \to 4^+$ transition and instead proposed a direct $5^- \to 2_1^+$ $E3$ decay [9]. The $5^- \to 4^+$ $E1$ strength reported in the former case would be similar to other transitions in this mass region, however, if the latter case were true, it would imply some unusual properties for this isomer. Notably, its $E3$ decay strength would be nearly an order of magnitude lower than any known $E3$ transition in the region, and its primary γ-decay energy would be the second largest of any known isomeric state, surpassed only by the decay of a core-excited $E4$ isomer in ^{98}Cd [10]. The disputed ^{32}Si decay scheme has also cast into doubt the energy of its 4_1^+ state, an important observable in even-even nuclei for testing *ab initio* models. A likely explanation for the isomerism of the 5^- state is that it is spin trapped due to being lower in energy than the 4_1^+ state, however, this could not be determined from the previous studies. We report new experimental data confirming the inverted ordering of the 5_1^- and 4_1^+ states in ^{32}Si, making it the lowest mass even-even nucleus known to contain a spin-trapped isomer.

Our experiment was performed at the ISAC-II facility of TRIUMF, where excited states of interest in ^{32}Si were populated using a ^{12}C(^{22}Ne, 2p) fusion-evaporation reaction with a ^{22}Ne beam energy of 2.56A MeV. The cross section of the ^{32}Si channel was approximately 0.6 mb, corresponding to ≈1.5% of the total data collected. γ rays were detected using the TIGRESS array [11] instrumented with 14 segmented HPGe clovers: four each at 45° and 135°, and six at 90° with respect to the beam axis. Charged particles were detected using a 128-channel spherical CsI(Tl) array [12]. Charged particle identification was performed using off-line pulse shape analysis [13] to separate the two-proton exit channel populating ^{32}Si. A self-supporting 500 μg/cm^2 $^{\text{nat.}}$C target foil produced by Micromatter [14] was used with a 23.6 mg/cm^2 Pb catcher foil mounted approximately 1 mm downstream. The purpose of the catcher foil was to stop ^{32}Si recoils before the decay of the isomer, allowing separation of prompt and isomeric transitions based on the Doppler shift. For lifetime measurements using the Doppler-shift attenuation method (DSAM), an alternate target consisting of a 394 μg/cm^2 layer of $^{\text{nat.}}$C on a 24 mg/cm^2 Pb backing was used [15].

Spins of states populated in ^{32}Si were determined from γ-ray directional correlation ratio (R_{DCO}) values [16], which were measured using two angular bins assigned to the TIGRESS clovers at 90°, and the TIGRESS clovers at 45° or 135°, respectively. For these angles, values of $R_{\text{DCO}} \approx 0.5$ are obtained for stretched dipole transitions and $R_{\text{DCO}} \approx 1.0$ for stretched quadrupole or octupole transitions, when gating on a coincident stretched quadrupole transition. Where sufficient statistics were available, the electric or magnetic character of transitions was determined using the polarization direction correlation method [17]. The measured polarization asymmetry Δ_{asym} was corrected for the intrinsic asymmetry in the response of TIGRESS measured using ^{56}Co source data. The validity of the above techniques was confirmed using transitions of known multipolarity in the ^{26}Mg side channel. Lifetimes of nonisomeric states were determined from a comparison of the DSAM target data to GEANT4-based simulations as described in Ref. [18] and previously implemented in Refs. [19,20]. Feeding corrections and estimations of

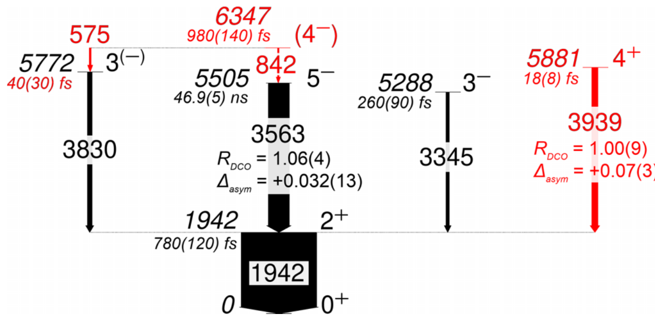

FIG. 1. Partial decay scheme of ^{32}Si, with R_{DCO} (gated on the $2_1^+ \to 0_1^+$ transition) and Δ_{asym} values listed for select transitions. Line widths indicate relative intensities of each transition. Newly observed levels and transitions and newly measured level lifetimes are in red.

systematic uncertainty due to the electronic stopping powers were performed using the methods of Ref. [20].

A partial decay scheme for ^{32}Si is shown in Fig. 1, with R_{DCO} and Δ_{asym} values listed for select transitions, as well as the mean lifetime measured for each level. Only levels and transitions necessary for identification and characterization of the isomeric state are shown. Additional states observed in this experiment will be presented in a future paper.

The ^{32}Si nanosecond isomer has previously been proposed at either 5581 keV [8] or 5504 keV [9]. In the former case, a 79(1) keV transition was reported between the proposed isomeric state and the 5504 keV level. In the present work we observe a delayed cascade depopulating a level at 5505.2(2) keV, but no coincident 79 keV transition, see Fig. 2. The intensity upper limit of a hypothetical stopped line at this energy was determined to be 1.2% relative to the fully stopped 3562.84(14) keV line, based on the Compton background at 79 keV and the relative γ-ray detection efficiency of TIGRESS at the energies of interest. Prior to background subtraction, a stopped line at 78 keV was observed corresponding

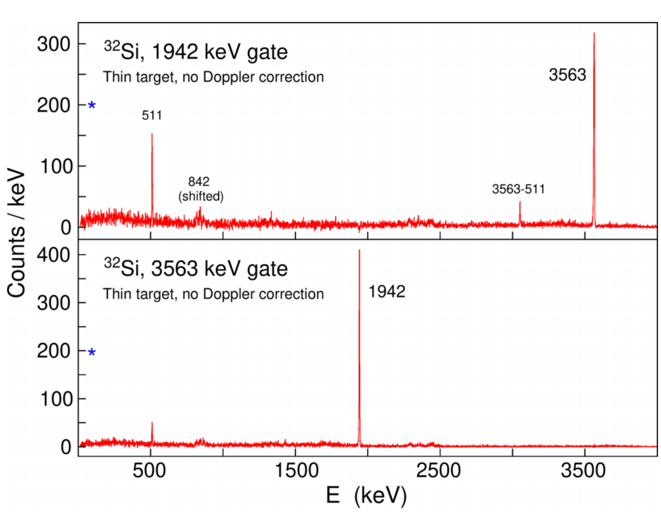

FIG. 2. Background subtracted γ-ray spectra gated on stopped lines in ^{32}Si. The expected position and height of a 79 keV member of the isomeric cascade is labeled with the "*" character.

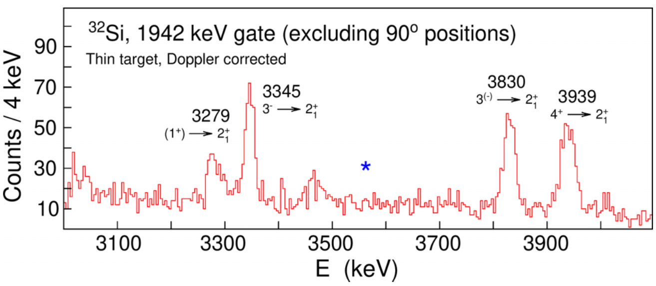

FIG. 3. Doppler-corrected γ-ray spectrum gated on the prompt component of the 1942.13(9) keV transition in ^{32}Si. The expected position of a prompt component of the 3562.84(14) keV transition is labeled with the "*" character.

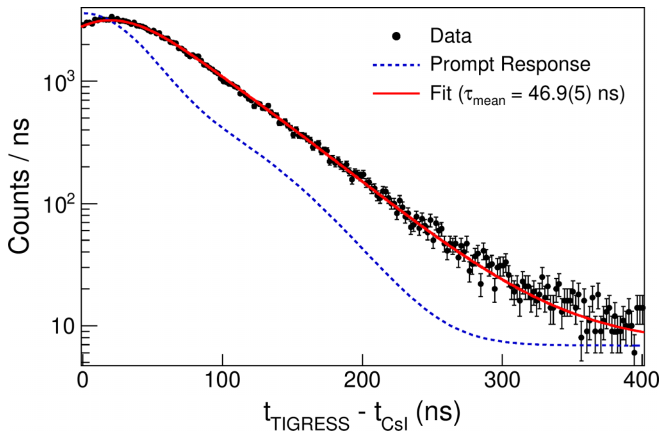

FIG. 4. Background subtracted TIGRESS-CsI timing distribution for the 3562.84(14) keV transition in ^{32}Si.

to time-random background from ^{32}P, which is very strongly populated in the ^{12}C(^{22}Ne, *pn*) side channel.

Since the 79 keV transition of Ref. [8] was not observed, we investigated the possible isomerism of the 5505.2(2) keV level based on its spin-parity and the observed decay scheme. The R_{DCO} and Δ_{asym} values of Fig. 1 strongly favor an $E2$ or $E3$ assignment for the 3562.84(14) keV transition, consistent with the $J^\pi = (5^-, 4^+)$ assignment for the parent level from previous ^{30}Si(t, p) data [21]. Given the large transition energy, only the 5^- case would produce an isomeric state. The excitation energy of the isomer was constrained based on the decays of a newly observed level at 6347.3(4) keV, depopulated via a 842.1(3) keV transition feeding the isomeric cascade, as well as a 574.9(3) keV transition to a side band outside of the isomeric cascade. Neither of the 574.9(3) or 842.1(3) keV lines is a member of the isomeric cascade, as they are not stopped in the thin target data. Comparing the total energies of each decay path from the 6347.3(4) keV level to the ground state, the energy of the isomeric state is constrained to 5505.3(14) keV, which agrees very well with the observed level at 5505.2(2) keV.

Despite the observed prompt feeding of the 5505.2(2) keV level, there was no observed prompt component of the 3562.84(14) keV transition depopulating this level. An upper limit on the intensity of an unobserved prompt component was estimated by gating on the Doppler-shifted component of the $2_1^+ \rightarrow 0_1^+$ transition (excluding detectors at 90° where the shifted and stopped energies overlap). The resulting spectrum is shown in Fig. 3 and contains no indication of a prompt 3562.84(14) keV transition. An intensity upper limit of 1.5% was derived for the prompt component of the 3562.84(14) keV transition relative to its stopped component, based on the Compton background intensity. This upper limit is four times lower than the observed prompt feeding from the 842.1(3) keV transition alone, and 35 times lower than the total intensity of all observed feeders of the 5505.2(2) keV level. Based on the large amount of prompt feeding to this level and the lack of a prompt component in its decay, we conclude that the 5505.2(2) keV level is isomeric and assign it $J^\pi = 5^-$.

The lifetime of this isomer was determined from the TIGRESS-CsI timing response, shown in Fig. 4. The prompt response consisted of background data in the energy range ±150 keV around the 3562.84(14) keV transition of interest, and was fit to a double Gaussian function to account for asymmetry of the timing peak. The full width at half-maximum of the prompt response was 78.8(4) ns. As this width was larger than the expected lifetime of the isomer, the isomer timing response was fit to the prompt response convoluted with an exponential decay function as described in Ref. [22]. The best fit lifetime was $\tau_{\mathrm{mean}} = 46.9(5)$ ns, consistent with the value of 47.8(7) ns reported in Ref. [9]. The isomer lifetime was also measured using γ-γ timing from the 842.1(3) and 3562.84(14) keV transitions, yielding a result of 44(4) ns, with the larger error in this measurement due to the lower statistics available following γ gating.

Our identification of the isomeric state contradicts the 4_1^+ assignment of Ref. [8], with no other 4_1^+ candidates previously identified. The yrast 4^+ state plays an important role in the decay of the isomer as it is one of the few states predicted to have both similar excitation energy and spin. We have identified a strong candidate for this level at 5881.4(13) keV, depopulated by an intense 3938.9(13) keV transition to the 2_1^+ level. The DCO ratio and positive Δ_{asym} value obtained for this transition strongly favor an $E2$ assignment. Based on the high intensity of this transition relative to other lines and the fusion-evaporation reaction used in this experiment, the parent 5881.4(13) keV level is likely yrast or near yrast, implying $J > 2$. We therefore assign $J^\pi = 4^+$ to this level. This is almost certainly the yrast 4^+ state, and its higher excitation energy compared to the 5^- state confirms the existence of a yrast trap in ^{32}Si.

This new experimental data significantly clarifies the level structure of ^{32}Si at intermediate excitation energies sensitive to the effects of cross-shell excitation. To interpret these findings, shell model calculations were performed using the FSU interaction [23] in the *psdpf* valence space, and the SDPF-MU interaction [24] in the *sdpf* valence space. Negative parity $1p1h$ (one-particle, one-hole) states were restricted to single-neutron excitation in the SDPF-MU calculations, while positive parity states were restricted to the *sd* shell for both models. A comparison of level energies is shown in Fig. 5. In general, the energies of positive parity states are similar between both models and consistent with experiment. For

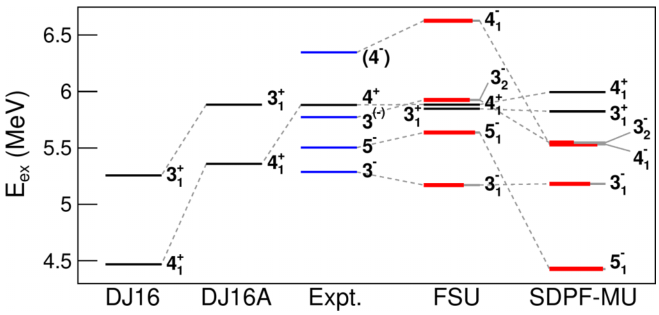

FIG. 5. Comparison of observed level energies to shell model calculations. For negative parity states, red bars indicate the calculated $\nu 0f_{7/2}$ orbital population.

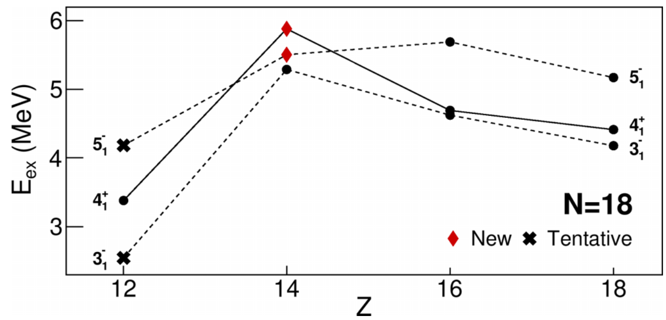

FIG. 6. Systematics of yrast states for $N = 18$ isotones in the vicinity of ${}^{32}_{14}$Si. Data from Refs. [31–34] and this work.

negative parity states, the SDPF-MU calculations appear to underpredict the energies of states with high neutron $0f_{7/2}$ occupancy, while the FSU calculations show better agreement. This agreement is unsurprising since the relevant two-body matrix elements of the FSU interaction are fitted to data in this mass region, with particular focus on negative parity states containing excitation to the $0f_{7/2}$ orbital [23]. Also shown in Fig. 5 are *ab initio* no-core shell model calculations using the DJ16 microscopic effective *sd* shell interaction [25] and the DJ16A interaction, which adds a phenomenological monopole modification to DJ16 [26], both constructed using the Okubo-Lee-Suzuki similarity transformation method [27]. The experimental data is better reproduced using the DJ16A interaction, with calculated 2_1^+ and 4_1^+ energies that are slightly lower than the experimental values, consistent with the results obtained for lighter *sd* shell nuclei [28].

The general agreement of the observed 4_1^+ energy with many model calculations across various valence spaces suggests that cross-shell excited configurations do not play a significant role in this state. In the DJ16A, FSU, and SDPF-MU calculations, the occupancy of either the $\pi s_{1/2}$ or $\pi d_{3/2}$ orbital is significantly higher for the 4_1^+ level compared to the lower-lying states, suggesting that the 4_1^+ energy is sensitive to the $Z = 14$ subshell closure. All models predict $B(E2; 4_1^+ \rightarrow 2_1^+)$ values consistent with our DSAM measurement, see Table I.

The isomer lifetime measurement yielded a $B(E3; 5_1^- \rightarrow 2_1^+)$ value of 0.0841(10) W.u., which is significantly hindered compared to any known $E3$ transition in this mass region. The closest analog is a similarly hindered $5_1^- \rightarrow 2_1^+$ $E3$ transition in ^{68}Ni, which has been attributed to its 5_1^- state being dominated by the $(\nu p_{1/2})^{-1} \otimes (\nu g_{9/2})^1$ configuration from $N = 40$ cross-shell excitation [29]. In ^{32}Si, a similar hindrance of the $E3$ strength seems to arise with the dominant $(\nu d_{3/2})^{-1} \otimes (\nu f_{7/2})^1$ configuration from $N = 20$ cross-shell excitation. The 5_1^- states calculated with FSU and SDPF-MU contain $\nu 0f_{7/2}$ occupancy factors of 0.92 and 0.96, respectively. The experimental $B(E3; 5_1^- \rightarrow 2_1^+)$ value is approximately halfway between the values calculated using these models. The differing configurations of the 5_1^- and 2_1^+ states sufficiently hinder this $E3$ transition such that the 5_1^- state is isomeric despite its unusually large γ-decay energy. A similar hindrance is evident for the unobserved $5_1^- \rightarrow 3_1^-$ branch as well as the unobserved $(4_1^-) \rightarrow 4_1^+$ and $(4_1^-) \rightarrow 3_1^-$ transitions, with the FSU and SDPF-MU calculations predicting significantly lower $\nu 0f_{7/2}$ occupancy for the 3_1^- state compared to the 4_1^- and 5_1^- states, as shown in Fig. 5.

Figure 6 shows a comparison of the present data to studies of other $N = 18$ isotones, indicating that the reordering of yrast states is specific to ${}^{32}_{14}$Si. The 4_1^+ level energy is enhanced at the $Z = 14$ subshell closure, which has been shown to widen with increasing neutron number [30]. For the negative parity states, both the FSU and SDPF-MU calculations show that the narrowing of the $N = 20$ shell gap becomes significant for $Z < 14$, and the FSU calculations show that mixed proton-neutron excitation to $0f_{7/2}$ becomes significant for $Z > 14$ (a likely explanation is that proton excitation to $0f_{7/2}$ becomes more energetically favorable with increased ground-state occupation of the upper *sd* orbitals). Both of these effects lower the energy of the 3_1^- and 5_1^- states, with the latter effect being stronger for the 3_1^- states. At $Z = 14$, the proton $0f_{7/2}$ contribution is mostly absent, with the FSU calculations showing an occupancy of 0.074 for the 3_1^- state in ${}^{32}_{14}$Si, compared to 0.325 in ${}^{34}_{16}$S. This reduces the energy gap between the 3_1^- and 5_1^- states in ^{32}Si, which suppresses the $5_1^- \rightarrow 3_1^-$ decay branch. The spin-trapped 5_1^- isomer therefore arises due to the varied effects of proton and neutron cross-shell excitation on different states in the yrast sequence.

In summary, the properties of the ^{32}Si isomeric state were determined, with the 4_1^+ state identified at higher energy. This shows that the isomer is located in a yrast trap, which forms due to the relevant yrast states containing different

TABLE I. Transition strength values measured in the present work, compared to model calculations. Effective charges $e_p = 1.36e$ and $e_n = 0.45e$ were used with all models.

		$B(\lambda L)$ (W.u.)				
$J_i^\pi \rightarrow J_f^\pi$	λL	Expt.	FSU	SDPF-MU	DJ16	DJ16A
$2_1^+ \rightarrow 0_1^+$	$E2$	$6.3^{+1.1}_{-0.8}$	7.3	6.3	12.4	10.1
$4_1^+ \rightarrow 2_1^+$	$E2$	8^{+7}_{-3}	11.2	8.2	15.2	11.4
$5_1^- \rightarrow 3_1^-$	$E2$	<0.053[a]	0.077	0.6	-	-
$5_1^- \rightarrow 2_1^+$	$E3$	0.0841(10)	0.150	0.012	-	-

[a]From intensity limit of unobserved transition.

configurations sensitive to proton and/or neutron cross-shell excitation. This is the only known case of a spin isomer in an even-even *sd* shell nucleus, and a rare example of an isomer with a very high γ-decay energy. High-spin isomers are best populated using fusion-evaporation reactions, however, many neutron-rich nuclides have yet to be studied in this way due to the challenge imposed by low reaction cross sections. Development of higher-intensity radioactive beams will help to address this challenge.

The authors appreciate the support of the ISAC Operations Group at TRIUMF and the Simon Fraser University Electronics and Machine Shops. This work was supported by the Natural Sciences and Engineering Research Council of Canada, the Canadian Foundation for Innovation, and the British Columbia Knowledge Development Fund. TRIUMF receives federal funding through a contribution agreement with the National Research Council of Canada. This work was also supported by the U.S. Department of Energy, Office of Science, Office of Nuclear Physics under Award No. DE-SC0020451 (FRIB), and by the U.S. Department of Energy Grant No. DE-FG02-93ER40789. FSU shell model calculations were performed using the computational facility of Florida State University, supported by Grant No. DE-SC0009883 (FSU). P.C.S. acknowledges financial support from SERB (India), CRG/2022/005167.

[1] T. Otsuka, T. Suzuki, R. Fujimoto, H. Grawe, and Y. Akaishi, Phys. Rev. Lett. **95**, 232502 (2005).
[2] E. K. Warburton, J. A. Becker, and B. A. Brown, Phys. Rev. C **41**, 1147 (1990).
[3] Y. Utsuno, T. Otsuka, T. Mizusaki, and M. Honma, Phys. Rev. C **60**, 054315 (1999).
[4] T. J. Gray, J. M. Allmond, Z. Xu, T. T. King, R. S. Lubna, H. L. Crawford, V. Tripathi, B. P. Crider, R. Grzywacz, S. N. Liddick, A. O. Macchiavelli, T. Miyagi, A. Poves, A. Andalib, E. Argo, C. Benetti, S. Bhattacharya, C. M. Campbell, M. P. Carpenter, J. Chan *et al.*, Phys. Rev. Lett. **130**, 242501 (2023).
[5] F. Rotaru, F. Negoita, S. Grévy, J. Mrazek, S. Lukyanov, F. Nowacki, A. Poves, O. Sorlin, C. Borcea, R. Borcea, A. Buta, L. Cáceres, S. Calinescu, R. Chevrier, Z. Dombrádi, J. M. Daugas, D. Lebhertz, Y. Penionzhkevich, C. Petrone, D. Sohler *et al.*, Phys. Rev. Lett. **109**, 092503 (2012).
[6] M. Robinson, P. Halse, W. Trinder, R. Anne, C. Borcea, M. Lewitowicz, S. Lukyanov, M. Mirea, Y. Oganessian, N. A. Orr, Y. Peniozhkevich, M. G. Saint-Laurent, and O. Tarasov, Phys. Rev. C **53**, R1465 (1996).
[7] S. Garg, B. Maheshwari, B. Singh, Y. Sun, A. Goel, and A. K. Jain, At. Data Nucl. Data Tables **150**, 101546 (2023).
[8] B. Fornal, R. Broda, W. Królas, T. Pawłat, J. Wrzesiński, D. Bazzacco, D. Fabris, S. Lunardi, C. Rossi Alvarez, G. Viesti, G. de Angelis, M. Cinausero, D. R. Napoli, and Z. W. Grabowski, Phys. Rev. C **55**, 762 (1997).
[9] M. Asai, T. Ishii, A. Makishima, M. Ogawa, and M. Matsuda, *Nanosecond Isomers in* ^{32,33}Si *and* ^{34}P (JAERI Tandem Annual Report, 2001), pp. 23–24.
[10] A. Blazhev, M. Górska, H. Grawe, J. Nyberg, M. Palacz, E. Caurier, O. Dorvaux, A. Gadea, F. Nowacki, C. Andreoiu *et al.*, Phys. Rev. C **69**, 064304 (2004).
[11] G. Hackman and C. E. Svensson, Hyperfine Interact. **225**, 241 (2014).
[12] J. Williams, C. Andreoiu, G. C. Ball, N. Bernier, M. Bowry, S. S. Bhattacharjee, C. Burbadge, R. Caballero-Folch, A. Chester, F. H. Garcia, A. B. Garnsworthy, S. A. Gillespie, G. Hackman, R. Henderson, B. Jigmeddorj, C. Jones, P. Kowalski, R. Lafleur, A. D. MacLean, M. Morrison *et al.*, Nucl. Instrum. Meth. Phys. Res. A **939**, 1 (2019).
[13] P. Voss, R. Henderson, C. Andreoiu, R. Ashley, R. A. E. Austin, G. C. Ball, P. C. Bender, A. Bey, A. Cheeseman, A. Chester, D. S. Cross, T. E. Drake, A. B. Garnsworthy, G. Hackman, R. Holland, S. Ketelhut, P. Kowalski, R. Krücken, A. T. Laffoley, K. G. Leach *et al.*, Nucl. Instrum. Meth. Phys. Res. A **746**, 87 (2014).
[14] Micromatter Technologies Inc., https://www.micromatter.com/, accessed: October 17, 2023.
[15] J. Greene, P. Voss, and K. Starosta, J. Radiol. Nucl. Chem. **299**, 1121 (2014).
[16] A. Krämer-Flecken, T. Morek, R. Lieder, W. Gast, G. Hebbinghaus, H. Jäger, and W. Urban, Nucl. Instrum. Meth. Phys. Res. A **275**, 333 (1989).
[17] K. Starosta, T. Morek, C. Droste, S. Rohoziński, J. Srebrny, A. Wierzchucka, M. Bergström, B. Herskind, E. Melby, T. Czosnyka, and P. Napiorkowski, Nucl. Instrum. Meth. Phys. Res. A **423**, 16 (1999).
[18] J. Williams, C. Andreoiu, R. Ashley, G. C. Ball, T. Ballast, P. C. Bender, C. Bolton, V. Bildstein, A. Chester, D. S. Cross, T. Domingo, T. Drake, A. Garnsworthy, P. Garrett, B. Hadinia, G. Hackman, R. Henderson, D. Jamieson, B. Jigmeddorj, A. Knapton *et al.*, Nucl. Instrum. Meth. Phys. Res. A **859**, 8 (2017).
[19] J. Williams, G. C. Ball, A. Chester, T. Domingo, A. B. Garnsworthy, G. Hackman, J. Henderson, R. Henderson, R. Krücken, A. Kumar, K. D. Launey, J. Measures, O. Paetkau, J. Park, G. H. Sargsyan, J. Smallcombe, P. C. Srivastava, K. Starosta, C. E. Svensson, K. Whitmore *et al.*, Phys. Rev. C **100**, 014322 (2019).
[20] J. Williams, G. C. Ball, A. Chester, P. Choudhary, T. Domingo, A. B. Garnsworthy, G. Hackman, J. Henderson, R. Henderson, R. Krücken, R. S. Lubna, J. Measures, O. Paetkau, J. Park, J. Smallcombe, P. C. Srivastava, K. Starosta, C. E. Svensson, K. Whitmore, and M. Williams, Phys. Rev. C **102**, 064302 (2020).
[21] H. T. Fortune, L. Bland, D. L. Watson, and M. A. Abouzeid, Phys. Rev. C **25**, 5 (1982).
[22] J.-M. Régis, H. Mach, G. S. Simpson, J. Jolie, G. Pascovici, N. Saed-Samii, N. Warr, A. Bruce, J. Degenkolb, L. M. Fraile, C. Fransen, D. G. Ghita, S. Kisyov, U. Koester, A. Korgul, S. Lalkovski, N. Mărginean, P. Mutti, B. Olaizola, Z. Podolyak *et al.*, Nucl. Instrum. Meth. Phys. Res. A **726**, 191 (2013).
[23] R. S. Lubna, K. Kravvaris, S. L. Tabor, V. Tripathi, E. Rubino, and A. Volya, Phys. Rev. Res. **2**, 043342 (2020).
[24] Y. Utsuno, T. Otsuka, B. A. Brown, M. Honma, T. Mizusaki, and N. Shimizu, Phys. Rev. C **86**, 051301(R) (2012).
[25] A. Shirokov, I. Shin, Y. Kim, M. Sosonkina, P. Maris, and J. Vary, Phys. Lett. B **761**, 87 (2016).

[26] N. A. Smirnova, B. R. Barrett, Y. Kim, I. J. Shin, A. M. Shirokov, E. Dikmen, P. Maris, and J. P. Vary, Phys. Rev. C **100**, 054329 (2019).
[27] K. Suzuki and R. Okamoto, Prog. Theor. Phys. **92**, 1045 (1994).
[28] P. Choudhary and P. C. Srivastava, Nucl. Phys. A **1033**, 122629 (2023).
[29] R. Broda, B. Fornal, W. Królas, T. Pawłat, D. Bazzacco, S. Lunardi, C. Rossi-Alvarez, R. Menegazzo, G. de Angelis, P. Bednarczyk, J. Rico, D. De Acuña, P. J. Daly, R. H. Mayer, M. Sferrazza, H. Grawe, K. H. Maier, and R. Schubart, Phys. Rev. Lett. **74**, 868 (1995).
[30] O. Bespalova, N. Fedorov, A. Klimochkina, M. Markova, T. Spasskaya, and T. Tretyakova, Eur. Phys. J. A **54**, 2 (2018).
[31] M. S. Basunia, Nucl. Data Sheets **111**, 2331 (2010).
[32] C. Ouellet and B. Singh, Nucl. Data Sheets **112**, 2199 (2011).
[33] N. Nica and B. Singh, Nucl. Data Sheets **113**, 1563 (2012).
[34] N. Nica, J. Cameron, and B. Singh, Nucl. Data Sheets **113**, 1 (2012).